



Cite this: DOI: 10.1039/d0ay01563f

# Real-time characterization of mammalian cell culture bioprocesses by magnetic sector MS†

Patrick Floris,<sup>a</sup> Noemí Dorival-García,<sup>a</sup> Graham Lewis,<sup>b</sup> Graham Josland,<sup>b</sup> Daniel Merriman<sup>b</sup> and Jonathan Bones<sup>a,c</sup>

Mammalian cell culture processes were characterized upon the analysis of the exhaust-gas composition achieved through the on-line integration of a magnetic sector MS analyser with benchtop bioreactors. The non-invasive configuration of the magnetic sector MS provided continuous evaluation of the bioreactor's exhaust gas filter integrity and facilitated the accurate quantification of O<sub>2</sub> and CO<sub>2</sub> levels in the off-gas stream which ensured preserved bioreactor sterility prior to cell inoculation and provided evidence of the ongoing cellular respiratory activity throughout the cultures. Real-time determination of process parameters such as the Respiratory Quotient (RQ) allowed for precise pin-pointing of the occurrence of shifts in cellular metabolism which were correlated to depletion of key nutrients in the growth medium, demonstrating the suitability of this technology for tracking cell culture process performance.

Received 17th August 2020  
Accepted 3rd November 2020

DOI: 10.1039/d0ay01563f

rsc.li/methods

## 1 Introduction

The complexity of mammalian cell culture processes for biopharmaceutical manufacturing has resulted in the rapid development of Process Analytical Technology (PAT) tools aimed at improving batch-to-batch reproducibility through the implementation of real-time process monitoring techniques.<sup>1–3</sup> In particular, on-line platforms can provide rapid access to key performance indicators (KPIs) and critical process parameters (CPPs) which can assist the operator's decision-making process and facilitate the timely implementation of required corrective actions.<sup>4,5</sup>

Cells have the ability to adjust their metabolic flux depending on specific culture conditions<sup>6,7</sup> and information on the consumed energy source can be obtained by monitoring shifts in respiratory profiles.<sup>8–11</sup> On-line measurement of key respiratory parameters, including the Carbon Dioxide Evolution Rate (CER), Oxygen Uptake Rate (OUR) and the ratio of these two parameters, the Respiratory Quotient (RQ), facilitated the implementation of adaptive feeding control strategies aimed at increasing yields in fungal<sup>12–14</sup> and bacterial<sup>15</sup> fermentation processes. However, the implementation of RQ as a practical process control tool in mammalian systems has been limited by the difficulties associated with its accurate

measurement, resulting in a broad range of reported values which varied depending on the cell line type and cultivation conditions.<sup>11</sup> The high solubility of CO<sub>2</sub> and the presence of bicarbonate buffer in the culture medium can introduce errors in the CER measurements.<sup>16,17</sup> Furthermore, headspace dilution effects may also introduce a delayed response in the exhaust gas signal which can potentially result in erroneous CER, OUR and RQ measurements.<sup>18,19</sup> Among all measurable respiratory parameters, OUR values have been preferentially implemented for the development of adaptive feeding control strategies in mammalian cell culture processes<sup>20–23</sup> since they can be accurately determined through global mass balance, liquid phase balance and dynamic method approaches as a result of poor O<sub>2</sub> solubility<sup>24,25</sup> while mathematical models have been reported to improve the accuracy of CER measurements by accounting for the liquid-gas transfer of CO<sub>2</sub> from bicarbonate as a function of pH variations in the culture medium.<sup>19,26</sup> However, the main bottleneck for accurate off-gas characterization in mammalian cultures is related to the low cell densities, resulting in relative small changes in O<sub>2</sub> and CO<sub>2</sub> concentrations which are difficult to quantify.<sup>26</sup>

Electronic noses based on metal oxide sensors have been historically adopted for on-line characterization of mammalian culture off-gas as exposure to volatile species produced a variation in the sensor's electrical response.<sup>8</sup> The low sensitivity, lack of selectivity and the need for chemometric interpretation of data rendered this technology inefficient as a PAT tool. Paramagnetic or electrochemical detectors were further implemented for on-line O<sub>2</sub> quantification in mammalian cell cultures while CO<sub>2</sub> measurements were obtained through potentiometric or non-dispersive IR (NDIR) detectors<sup>17,19,26</sup> which can be configured to monitor a single gas sample stream,

<sup>a</sup>Characterisation and Comparability Laboratory, NIBRT-The National Institute for Bioprocessing Research and Training, Fosters avenue, Mount Merrion, Blackrock, Co. Dublin, A94 X099, Ireland. E-mail: jonathan.bones@nibr.ie

<sup>b</sup>Thermo Fisher Scientific, Ion Path, Road Three, Winsford, CW7 3GA, UK

<sup>c</sup>School of Chemical and Bioprocess Engineering, University College Dublin, Dublin 4, Belfield, D04 V1W8, Ireland

† Electronic supplementary information (ESI) available. See DOI: 10.1039/d0ay01563f

either the inlet or outlet gas line from the bioreactor, or can perform analysis of alternated inlet and outlet streams through line multiplexing. Simultaneous monitoring of multiple bioreactors required during process development operations would therefore require an unpractical equivalent number of stand-alone detectors. Despite showing promising performance for real-time mammalian bioprocess monitoring, paramagnetic and NDIR detectors are limited by slow sampling speed, narrow operating range and low accuracy, which is typically  $\pm 0.2\%$  (v/v) for  $O_2$  and  $\pm 2\%$  (v/v) for  $CO_2$ .<sup>17,19</sup>

Mass spectrometers can provide improved sensitivity for off-gas analysis which facilitates the detection of physiological changes in animal cell bioprocesses characterized by low respiratory activity.<sup>27</sup> Quadrupole analysers have been implemented for real-time CER-OUR determination in CHO cell cultures<sup>20</sup> and RQ estimations in hybridoma cultivations.<sup>28</sup> In this study, we evaluated a magnetic sector MS gas analyser as a tool for real-time monitoring of CHO cell cultivation processes. Despite the previous integration of magnetic sector MS for monitoring hybridoma<sup>29</sup> and CHO cell cultures,<sup>27</sup> recent developments have occurred particularly with regard to sampling methodologies which facilitate the analysis of multiple gas streams within a matter of minutes using a single MS analyser, thereby potentially allowing simultaneous monitoring of multiple bioreactors which traditionally limited the integration of paramagnetic and NDIR exhaust-gas analysers during process development stages. Furthermore, magnetic sector analysers provide improved stability relative to quadrupole counterparts,<sup>30</sup> featuring characteristic flat top peaks which do not yield variations in signal intensities upon occurrence of small mass drifts, therefore being particularly advantageous for long-term process monitoring applications. The performance of the MS gas analyser was assessed throughout multiple bioprocessing stages, from pre-inoculation of the bioreactor to culture harvest, by evaluating batch and fed-batch mammalian cell cultures performed in benchtop bioreactors which were subjected to alteration in processing parameters aimed at establishing the suitability of magnetic sector MS as an effective real-time process monitoring technology.

## 2 Materials and methods

### 2.1 Determination of respiratory parameters by magnetic sector MS

A Prima BT magnetic sector MS benchtop system (Thermo Fisher Scientific, Winsford, UK) operated through the GasWorks 3.0 software package was implemented for direct sampling of headspace off-gas from mammalian CHO cell culture processes. The initial set up of the MS analyser involved running a 100% (v/v) He stream (BOC Gases Ireland, p/n 379-V) to rule out the presence of leaks in the transfer lines which could result in MS contamination, followed by 20% (v/v)  $CO_2$  in Ar (BOC Gases Ireland, p/n 225765-V-C) and a standard calibration air mixture comprising of 1% (v/v) Ar, 10% (v/v)  $CO_2$ , 22% (v/v)  $O_2$  and 67% (v/v)  $N_2$  (BOC Gases Ireland, p/n 149624-AV-G). A single MS calibration was performed due to the high signal stability provided by the instrument which provided high

measurement precision, determined for  $O_2$  to be 0.002–0.003% (v/v) over a 7 day monitoring period. Gas streams were introduced into the MS through the 16-port Rapid Multi-Stream Sampler (RMS), an optically-encoded rotating stream selector and analysed for  $CO_2$ ,  $O_2$ ,  $N_2$  and Ar with sample measurements taken every 30 seconds for each stream. Gas flow-rates reaching the detector were obtained through a sensor positioned within the RMS which provided measurements with an accuracy of  $\pm 12 \text{ mL min}^{-1}$ . The RMS was maintained at 60 °C during operation. The GasWorks software calculated the CER, OUR and the RQ values determined from their ratio (not reported) as defined in eqn (1)–(3) respectively, upon characterization of the gas supplied to the bioreactor (inlet) and of the exhaust-gas released from the vessel (outlet), as illustrated in Fig. 1.

$$\text{CER} = (\text{CO}_2\text{out} \times \text{flow-out}) - (\text{CO}_2\text{in} \times \text{flow-in}) \quad (1)$$

$$\text{OUR} = (\text{O}_2\text{in} \times \text{flow-in}) - (\text{O}_2\text{out} \times \text{flow-out}) \quad (2)$$

$$\text{RQ} = \text{CER}/\text{OUR} \quad (3)$$

The measurement of  $N_2$  which is inert relative to the cellular respiration process since it is not consumed or produced, facilitated the definition of the balance shown in eqn (4).

$$(\text{N}_2\text{in} \times \text{flow-in}) = (\text{N}_2\text{out} \times \text{flow-out}) \quad (4)$$

The limited accuracy of flow-meters is known to introduce errors in the calculation for RQ. Hence, eqn (4) was resolved for flow-out, yielding eqn (5), which facilitated the rearrangement of eqn (1) and (2) to allow the determination of the reported flow-corrected CER-OUR values, defined by GasWorks as CDC and OXC as shown in eqn (6) and (7) respectively, and of the RQ values as illustrated in eqn (8) which were reported for the experiments performed.

$$\text{Flow-out} = (\text{N}_2\text{in} \times \text{flow-in})/\text{N}_2\text{out} \quad (5)$$

$$\text{CDC} = [\text{CO}_2\text{out} \times (\text{N}_2\text{in}/\text{N}_2\text{out})] - \text{CO}_2\text{in} \quad (6)$$

$$\text{OXC} = \text{O}_2\text{in} - [\text{O}_2\text{out} \times (\text{N}_2\text{in})/(\text{N}_2\text{out})] \quad (7)$$

$$\text{RQ} = \text{CDC}/\text{OXC} \quad (8)$$

The respiratory profiles based on the CDC, OXC and RQ values for the batch culture identified as B-1 were reported upon averaging measurements within 30 minute sampling intervals. For the remaining cultures described, averaged values from 6 hour sampling intervals were reported instead. Colour coded error bars were included in the graphical representations which were representative of the obtained standard deviation.

### 2.2 On-line integration of magnetic sector MS analyser with benchtop bioreactors

Two distinct configurations were evaluated for the on-line integration of the magnetic sector MS analyser with 3 L and 7 L total volume Thermo Fisher HyPerforma glass bioreactors

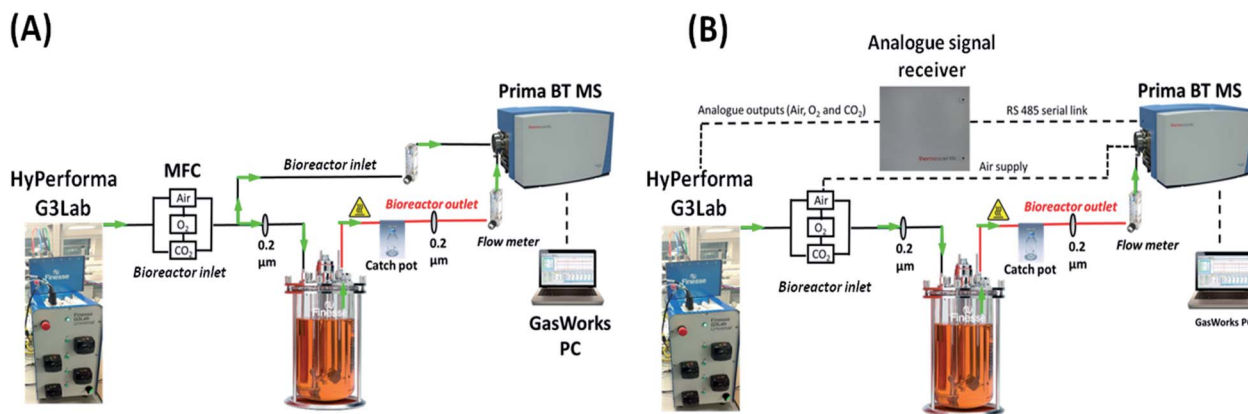


**Fig. 1** Schematics showing the implemented on-line integration of a magnetic sector MS with a benchtop bioreactor. The inlet gas supplied to the culture was characterized upon (A) the diversion of a portion of the flow delivered by the MFC towards the MS prior to entering the bioreactor and (B) analogue transfer of inlet gas-flow rate parameters from the HyPerforma G3Lab controller to the GasWorks software. A separate line was run in configuration B from the air supply directly to the MS analyser.

(Thermo Fisher Scientific, MA, USA), controlled by a Thermo Fisher HyPerforma G3Lab Universal controller and operated using the TruBio DeltaV software V5.0.0. The initial configuration, defined as V1 and shown in Fig. 1(A), involved a diversion of the inlet gas supplied from the mass flow controller (MFC) towards the MS prior to entering the bioreactor through a barbed t-piece connector (p/n 06294-10, Cole-Parmer, IL, USA) using low-permeability C-Flex 374 tubing (Saint-Gobain, Courbevoie, France) with dimensions of 4.8 mm internal diameter (I.D.)  $\times$  8 mm outer diameter (O.D.)  $\times$  1.5 m (length) to allow transfer of the gas streams. Similarly, the off-gas stream was directed to the RMS of the mass spectrometer by running a heated line using tubing of identical dimensions from a single overlay port positioned on the vessel's head plate. A 500 mL catch-pot with a twin-hose cap (p/n 15193927, Fisher Scientific, Dublin, Ireland) was introduced to collect condensate build-up on the outlet heated line and flow-meters (p/n 198-2975, Radionics, Dublin, Ireland) integrated prior to the RMS facilitated both inlet and outlet gas flow-rate adjustments. Sterility within the bioreactor was preserved through the integration of a single 0.2  $\mu\text{m}$  PTFE vent filter, either 37 mm Acro 37 TF (Pall, NY, USA) or 50 mm ReZist Air (GE Healthcare, IL, USA), positioned immediately after the catch-pot container along the outlet line. The second MS-bioreactor configuration, defined as V2 and shown in Fig. 1(B), involved the analogue transfer of individual gas flow-rate values from the Thermo Fisher G3Lab system auxiliary ports to GasWorks which calculated in real-time the composition of the inlet gas stream supplied from the ratio of these parameters and from the composition of air which was determined by MS upon running a gas transfer line directly from the air supply to the detector. The flow path for exhaust-gas analysis remained unaltered in the V2 configuration.

### 2.3 Bioreactor sterility assessment

A 7 L total volume bioreactor vessel was subjected to porous steam-sterilization at 121  $^{\circ}\text{C}$  followed by aseptic filling with 3 L of liquid BalanCD growth A medium (Irvine Scientific, CA, USA)

containing 2.2 g  $\text{L}^{-1}$  sodium bicarbonate. An agitation rate of 188 rpm was set and a steady gas stream comprising of 0.3  $\text{L min}^{-1}$  air and 0.020  $\text{L min}^{-1}$   $\text{CO}_2$  was delivered from the G3Lab MFC to the vessel through a ring macro-sparger. The composition of the exhaust gas was determined by the Prima BT MS system which was interfaced with the 7 L vessel through the V1 configuration. An increase in temperature from 25  $^{\circ}\text{C}$  to 37  $^{\circ}\text{C}$  after 110 hours was introduced from the start of the experiment. Baseline measurements were determined between 150–200 hours by monitoring signal stability for  $\text{O}_2$  and  $\text{CO}_2$  from off-gas measurements acquired by MS and *in situ* pH-%  $\text{dO}_2$  measurements determined every 30 seconds through a TrupH and a TruDO probes (Thermo Fisher Scientific, MA, USA). Bioreactor contamination was deliberately introduced at 204 hours through the removal of the TruDO probe for 30 seconds which was subsequently re-inserted into the vessel. Baseline variations in signal responses for  $\text{O}_2$  and  $\text{CO}_2$  greater than  $3\times$  times the corresponding standard deviation values from each measurement technique were considered to be clear signs of contamination as visualized after 204 hours.

### 2.4 Mammalian cell culture process conditions

A CHO-K1 cell line producing a humanized IgG1 monoclonal antibody was initially cultured in shake-flasks within a humidified incubator kept at 37  $^{\circ}\text{C}$  with 5% (v/v)  $\text{CO}_2$  and an agitation rate of 120 rpm using chemically defined BalanCD growth A liquid medium which was further supplemented with 1.2–1.7 g  $\text{L}^{-1}$  L-glutamine (Sigma-Aldrich, Dublin, Ireland). The cell seeding density upon vial thawing was  $0.3 \times 10^6$  cells per  $\text{mL}^{-1}$  in 250 mL total volume Erlenmeyer polycarbonate flasks (Corning, NY, USA). A cell seeding density of  $0.8 \times 10^6$  cells per  $\text{mL}^{-1}$  was maintained through regular passaging every 2 days once densities of 3 to  $4 \times 10^6$  cells per  $\text{mL}^{-1}$  were reached. The cells were transferred after two weeks of continuous passaging into four 1 L total volume polycarbonate shake-flasks which were used as inoculum for bioreactor cultivations. Batch and fed-batch cultures, identified as B-x and FB-x cultures

respectively, were performed in the Thermo Fisher HyPerforma vessels integrated with the MS analyser through both V1 and V2 on-line configurations as summarized in Table 1. Bioreactors were inoculated at densities of  $0.8 \times 10^6$  cells per  $\text{mL}^{-1}$  and maintained at  $37^\circ\text{C}$ . Mixing was performed through single 3-blade marine type impellers at stirring rates of 200 rpm for 3 L scale, 2 L medium working volume, and 188 rpm for 7 L scale, 5 L medium working volume, achieving  $k_{\text{La}}$  value of 4 and  $3 \text{ h}^{-1}$ , respectively, as determined by the dynamic gassing out method performed with  $0.5 \text{ L min}^{-1}$  air flow-rates. A prototype liquid feed supplied by Irvine Scientific was supplemented in fed-batch cultures performed at 7 L scale only, involving 6% (v/v) additions of the initial 3.5 L culture volume after 48, 72, 96, 168 and 216 culture hours. Individual streams of air,  $\text{O}_2$  and  $\text{CO}_2$  were supplied from pressurized cylinders at 2 bar to the G3Lab MFC which delivered a combined gas stream to the liquid medium through a L-pipe sparger at 3 L scale and a ring sparger at 7 L scale. A number of culture process parameters were varied during fed-batch processes to evaluate the performance of the magnetic sector MS analyser including: the implementation of a temperature drop from  $37^\circ\text{C}$  to  $32^\circ\text{C}$  at 144 culture hours in the culture FB-2, bolus glucose additions at 120 and 144 culture hours in the culture FB-3 to maintain levels at approximately  $5 \text{ g L}^{-1}$  and the introduction of rapid fluctuations in  $\text{O}_2$  flow-rates supplied to culture FB-4 aimed at maintaining %  $\text{dO}_2$  saturation levels between 40–50%. Neutralization of culture pH was achieved in fed-batch cultures by automatic additions of  $\text{CO}_2$  and 1 M NaOH while foaming was controlled with 2% (v/v) Antifoam C emulsion (Sigma-Aldrich, Ireland) which was added as needed.

### 2.5 Off-line measurement of cell culture parameters

Bioreactor sampling preceded bioreactor feeding and involved daily collection of 5 mL volume samples which were analysed off-line using a BioProfile FLEX 2 analyzer (Nova Biomedical, MA, USA) providing concentrations for glucose, lactate, glutamine, % cell viability and viable cell density. Antibody titer was determined by affinity chromatography on an Ultimate 3000 LC system (Thermo Fisher Scientific, MA, USA) with UV detection at 280 nm involving  $20 \mu\text{L}$  injections of cell culture supernatant on a  $4 \times 35 \text{ mm}$  MabPac protein A column (p/n 082539, Thermo Fisher Scientific, MA, USA) maintained at  $25^\circ\text{C}$ . Gradient conditions involved pumping 100%  $1 \times \text{PBS}$  (p/n 12821680, Fischer Scientific, Dublin, Ireland) at pH 7.0 until 0.9 minutes at a flow-rate of  $0.6 \text{ mL min}^{-1}$  followed by a switch to 100%  $1 \times \text{PBS}$  with 30 mM HCl at pH 2.0.

## 3 Results and discussions

### 3.1 Off-gas analysis for the determination of bacterial contamination

Contamination events result in considerable productivity losses for biopharmaceutical companies as affected batches become essentially unusable. Sterility must be preserved through all bioprocessing stages to ensure product purity as microbial species can replicate within the same nutrient-rich temperature controlled environments. The potential sources of process contamination are multiple, ranging from inefficient sterilization conditions to inadequate aseptic techniques implemented by operators. Furthermore, contaminants can access through cracks formed within welded sample lines or seals which might not be always readily detectable or preventable. Unjustified variations in medium pH and %  $\text{dO}_2$  measurements are considered to be the standard approach for establishing the presence of bacterial contaminants<sup>31</sup> however, analysis of the exhaust gas can be equally effective for detecting the presence of undesired respiratory activity while being minimally invasive. For this purpose, profiles for  $\text{O}_2$  and  $\text{CO}_2$  were determined in real-time from the off-gas released from a 7 L benchtop bioreactor filled aseptically with culture medium. Subsequently, deliberate alteration of the sterile barrier was performed in effort to establish the efficacy of MS analysis for rapid detection of contamination. The integration of the bioreactor with the MS analyser was achieved through an on-line configuration, defined as V1 and shown in Fig. 1(A), which involved diverting a portion of the inlet gas supplied to the bioreactor towards the RMS for compositional characterization. Off-gas measurements were correlated with pH and %  $\text{dO}_2$  values obtained from probes displaced *in situ* within the medium while preserving measurement consistency among all the techniques evaluated upon adjustment of the read-out frequency to 30 seconds. The rapid multi-stream sampling (RMS) configuration of the magnetic sector MS analyser facilitated automatic analysis of up to 16 different gas streams, therefore potentially allowing simultaneous monitoring of 8 bioreactors based on the implemented configuration, upon correlating the composition of the gas supplied to individual cultures with a corresponding off-gas profile. However, only two streams were monitored in this study involving the inlet and outlet gas streams of a single bioreactor to illustrate proof of concept. The cycling time, which is the time required for the RMS to sequentially sample all the configured gas streams and return to the original sampling point, was 1 minute but could be decreased further to 20

**Table 1** Summary of mammalian cell cultures, and corresponding implemented process conditions, which were evaluated upon characterization of the exhaust-gas composition by magnetic sector MS

Culture ID	Culture mode	Working volume (L)	Headspace volume (L)	MS on-line configuration	Air ( $\text{L min}^{-1}$ )	$\text{O}_2$ ( $\text{L min}^{-1}$ )	$\text{CO}_2$ ( $\text{L min}^{-1}$ )
B-1	Batch	2.0	1.0	V1	0.3	N/a	0.016
FB-1	Fed-batch	3.5–5.0	3.5–2.0	V1	0.5	0–0.1	0–0.25
FB-2	Fed-batch, temperature drop	3.5–5.0	3.5–2.0	V2	0.5	0–0.1	0–0.25
FB-3	Fed-batch, glucose fed	3.5–5.0	3.5–2.0	V2	0.5	0–0.1	0–0.25
FB-4	Fed-batch, $\text{dO}_2$ 40–50%	3.5–5.0	3.5–2.0	V2	0.1–0.15	0–1.0	0–0.25

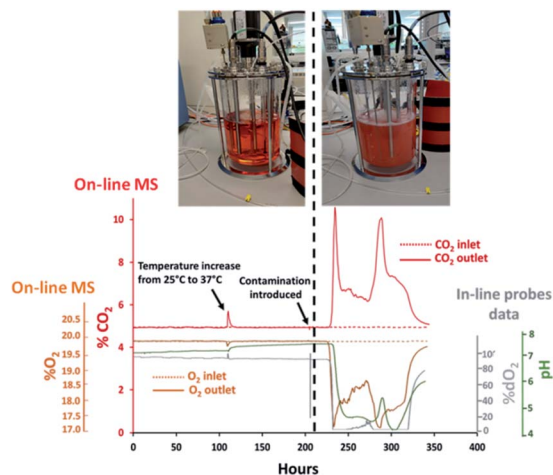


Fig. 2 Overview of off-gas profiles, determined by magnetic sector MS, and pH/% dO<sub>2</sub> values obtained *in situ* for the detection of medium contamination in a 7 L bioreactor. Sterility was preserved until 204 hours after which contamination was deliberately introduced.

seconds by adjustment of the read-out frequency to 10 seconds for each stream without compromising on measurement accuracy. A temperature increase of the culture medium from 25 °C to 37 °C was performed at 110 hours to replicate conditions typically implemented to commence medium holding stages, which decreased the solubility of CO<sub>2</sub> dissolved within the medium<sup>32</sup> and produced a sudden rise in the off-gas CO<sub>2</sub> levels detected by MS at this time point as shown in Fig. 2. Signal stability for all measurement techniques was visualised between 150–200 hours from initialization of the medium holding studies since stable process conditions were present during this time interval involving constant aeration supplemented with ~5% (v/v) CO<sub>2</sub>, aimed at maintaining pH values within the medium close to neutrality. The CO<sub>2</sub> contribution from the bicarbonate component in the medium at neutral pH conditions was expected to be negligible<sup>33</sup> as confirmed by the identical and stable signal measurements obtained in this time range from the analysis of the inlet gas supplied to the medium and of the exhaust-gas outlet streams with a composition of 19.80 ± 0.01% (v/v) for O<sub>2</sub> and 4.90 ± 0.02% (v/v) for CO<sub>2</sub>. Probes placed *in situ* provided further evidence of the presence of stable and contaminant-free conditions with corresponding dO<sub>2</sub> measurements of 97.82 ± 0.14% and pH values of 7.20 ± 0.01. Process measuring probes can often provide an access route for contaminants as damage can occur within O-rings seals due to repetitive over-tightening and exposure to elevated sterilization temperatures. Surface deformations on the damaged O-rings can form “pockets”, facilitating the deposit of particulates which can be shielded from sterilization.<sup>34</sup> However, contamination events due to seal damage are challenging to reproduce and further conditions can contribute to successful migration of micro-organisms into the vessels such as unfavourable differential pressures between the inner vessel and surrounding unsterile environment. The dO<sub>2</sub> probe was deliberately manipulated for the purpose of this study at 204 hours by creating an

Table 2 Time intervals required for the detection of culture medium contamination in a 7 L bioreactor based on MS off-gas analysis and pH/dO<sub>2</sub> parameters monitored through standard probes displaced *in situ*

	Contamination detection time (hours)
In-line % dO <sub>2</sub>	22.6
In-line pH	25.8
Off-gas O <sub>2</sub>	22.4
Off-gas CO <sub>2</sub>	23.7

opening through temporary detachment, approximately 30 seconds, from the headplate and exposing its outer surface to the unsterile outer environment to force medium contamination upon its reinsertion into the vessel. Signal stability was subsequently monitored and consistent shifts in both in-line and off-gas on-line measurements from the corresponding signal baseline greater than 3 times standard deviation values were considered to be clear indication of contamination. Good correlation for the determination of microbial contamination based on MS detection and % dO<sub>2</sub> values determined *in situ* was established since both approaches confirmed the presence of micro-organism induced respiratory activity within a ~1 hour time frame difference as summarized in Table 2. A rapid decrease in %O<sub>2</sub> values from the off-gas induced by micro-organism respiration was visualised after 22.4 hours from the removal of the dO<sub>2</sub> probe, with corresponding increases in off-gas %CO<sub>2</sub> values observed at 23.7 hours, and from the equally rapid decrease in % dO<sub>2</sub> determined *in situ* after 22.6 hours followed by increased medium turbidity. Bacteria growth produced a characteristic drop in pH<sup>35</sup> which however occurred at later intervals, after 25.8 hours. A 5.70% (v/v) increase in CO<sub>2</sub> levels was observed at 235 hours from the analysis of the off-gas composition which was considerably higher than a corresponding decrease of 2.50% (v/v) determined for O<sub>2</sub>, therefore unlikely to be related exclusively to bacteria cell respiratory activity. The rapid drop in pH induced by bacteria growth shifted the carbonate system equilibrium, which was converted almost entirely into CO<sub>2</sub>, therefore presumably resulting in excess quantities of CO<sub>2</sub> released into the off-gas. The subsequent decrease in off-gas CO<sub>2</sub> levels occurred as anticipated upon pH stabilization<sup>36</sup> since the carbonate equilibrium shifted CO<sub>2</sub> back to the HCO<sub>3</sub><sup>-</sup> form, producing a measured baseline increase for CO<sub>2</sub> of 1.40% (v/v), and a corresponding 1.30% (v/v) decrease in O<sub>2</sub> levels at 260 hours which was clearly more representative of micro-organism respiratory activity. Off-gas measurements ultimately facilitated the visualization of bacteria death at 340 hours as the composition of the exhaust gas returned to baseline levels with the simultaneous rapid increase in pH and % dO<sub>2</sub> saturation.

### 3.2 Real-time monitoring of batch CHO cell culture processes

The implementation of PAT tools during upstream bioprocessing stages must result in the real-time visualization of process related events for rapid detection of deviations. The

simplest approach for off-gas characterization involves correlating experimentally obtained off-gas measurements with performance indicators and process parameters, specifically viable cell density values and key nutrients or metabolites known to impact cell growth. The preliminary evaluation of the magnetic sector MS as a tool for real-time mammalian cell culture monitoring involved profiling the off-gas composition from a batch culture based on an antibody producing CHO-K1 cell line which was performed in a 3 L total volume bioreactor integrated on-line with the magnetic sector MS analyser through the previously described V1 configuration shown in Fig. 1(A). Steady state aeration conditions were implemented throughout the process without maintaining set pH and % dO<sub>2</sub> values which would otherwise require the introduction of variable process inputs with a potential impact on off-gas measurements. A medium hold study was initiated 24 hours prior to cellular inoculation to ensure the preservation of a sterile environment within the bioreactor, confirmed upon the visualization of inlet and off-gas profiles at the outlet with identical composition as shown in Fig. 3(A). Clear visualization of cellular respiratory activity during the lag phase was detectable from off-gas profiles as soon as 8 hours post CHO cell inoculation as a result of the high sensitivity provided by the magnetic sector MS analyser. A viable density of  $1.2 \times 10^6$  cells per mL<sup>-1</sup> was determined at this time point from off-line cell count measurements which correlated with a 0.03% (v/v) increase in CO<sub>2</sub> levels and a corresponding decrease of 0.04% (v/v) in O<sub>2</sub> levels detected from off-gas measurements. The observed changes in the off-gas composition were attributed to cellular respiration as a result of the implemented stable aeration conditions and of the minimal variations in pH values which remained close to neutrality at this time point. A considerable increase in the levels of CO<sub>2</sub> released into the off-gas was observed during the exponential cell growth phase which occurred between 24–120 culture hours, with a corresponding drop in O<sub>2</sub> levels, facilitating the clear visualization of the cellular transition state from the logarithmic growth phase

to the stationary phase at 100 culture hours which ultimately yielded the greatest detected variations for O<sub>2</sub> and CO<sub>2</sub> from off-gas measurements. Stoichiometric balance between the levels of O<sub>2</sub> consumed and CO<sub>2</sub> produced was observed at this time point, which varied by 0.65% (v/v) for each species, confirming that any potential CO<sub>2</sub> contributions from the bicarbonate medium component were unlikely to be significant at the measured pH of 6.6. A rapid decline of measured CO<sub>2</sub> levels in the off-gas was observed as cell death occurred after 200 culture hours with a consequent increase in O<sub>2</sub> values since this was no longer consumed for respiration. An equally significant rise in % dO<sub>2</sub> and in pH values was observed at this time point due to the corresponding increase in O<sub>2</sub> medium saturation and cell-induced consumption of accumulated lactate. Ultimately, the observed CO<sub>2</sub> profile determined from off-gas analysis closely resembled the cell growth curve derived from traditional off-line cell counting techniques while an inverse trend was observed for O<sub>2</sub> once consumed as a consequence of cellular respiration. Furthermore, the real-time estimation of the respiratory parameters CDC, OXC and the ratio of these, the RQ values, provided insight on variations in substrate consumption trends as illustrated in Fig. 3(B). A predominantly dominant carbohydrate-induced cell metabolism was observed from the estimation of RQ values close to the unity between 25–100 culture hours, matching a previously reported profile observed in DG44 CHO cell processes.<sup>19</sup> However, a clear divergence between CDC and OXC values was observed from 125 culture hours onwards indicative of a metabolic switch which produced a decreased RQ value of 0.8 at this time point. Off-line metabolite measurements facilitated correlation of the observed decrease in RQ value with the depletion of two major substrates required for mitochondrial energy production activity, specifically glutamine and glucose,<sup>37</sup> and a switch in lactate metabolism which was consumed rapidly until 300 hours when a drop in cell viability occurred as confirmed by the measured RQ value of 0 at this point indicative of the absence of cellular respiration.

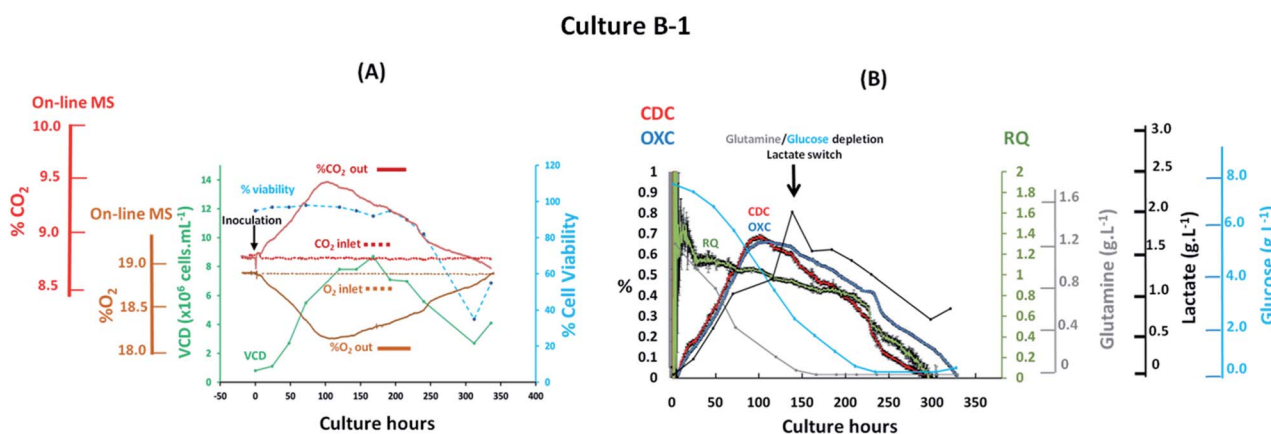


Fig. 3 Profiles of a batch CHO-K1 cell culture, identified as B-1, illustrating (A) the correlation between off-gas respiratory profiles, obtained by magnetic sector MS, cell growth profiles obtained from off-line measurements; (B) overlay of CDC, OXC and RQ values, obtained by magnetic sector MS, with nutrient/metabolite data obtained from off-line measurements. Respiratory CDC, OXC and RQ data was averaged from measurements at 30 minute intervals and error bars from standard deviations were included.

### 3.3 Impact of feed additions on off-gas profiles

The performance of the magnetic sector MS was subsequently evaluated upon the implementation of process variables in fed-batch cultures performed at 7 L scale involving the previously evaluated CHO-K1 cell line. The addition of nutrients performed at defined feeding intervals, which impacted the medium's ionic strength/osmolality, and the implementation of shifts in temperature during the stationary cell growth phase were likely to affect gas solubility in the medium and affect the off-gas profiles obtained. Furthermore, rapid variations of the inlet gas composition supplied to the cultures were implemented, as shown from the G3Lab profiles in the ESI Fig. S1,† producing variations in gas mass transfer which were likely to complicate accurate off-gas characterization, particularly for CO<sub>2</sub> as a result of its high solubility.<sup>17</sup> The supplementation of O<sub>2</sub> was performed to sustain % dO<sub>2</sub> values in the medium and preserve aerobic conditions desirable for extending cell viability<sup>38</sup> while additions of base titrant and CO<sub>2</sub> were introduced to maintain physiological pH values.<sup>39</sup> It was evident from the fed-batch culture FB-1 shown in Fig. 4(A) that O<sub>2</sub> supplementation, which increased its concentration from 19% (v/v) to 34% (v/v) during the initial 87 hours of the culture, rendered the visualization of respiratory activity from off-gas profiles challenging, particularly during the lag and logarithmic growth phases. Here, cell growth was preferentially tracked by monitoring variations in CO<sub>2</sub> levels since here the observed concentration shifts were considerably lower than what observed for O<sub>2</sub>, decreasing from 8.40% (v/v) to 1.40% (v/v) in the gas supplied to the bioreactor during the initial 48 culture hours. The observed drop in CO<sub>2</sub> levels occurred as a consequence of cell-induced lactate accumulation, confirmed by off-line measurements, which decreased the pH and minimized further CO<sub>2</sub> supplementation requirements. A 0.4% (v/v) variation in CO<sub>2</sub> between inlet and outlet profiles was detected at 48 culture hours however, it was not possible to attribute this variation entirely to cellular respiration as potential

contributions induced by mass transfer variations could have also contributed as a consequence of the variable gas supply introduced into the culture. Therefore, the composition of the inlet gas supplied to the culture was subsequently stabilized by limiting the supplemented O<sub>2</sub> flow-rate to 0.1 L min<sup>-1</sup> from 87 to 120 culture hours, corresponding to the stationary phase of the cell growth curve, to facilitate the clear visualization of cellular respiratory activity during this period as confirmed by a 0.6% (v/v) concentration difference between inlet and outlet signals for both O<sub>2</sub> and CO<sub>2</sub>. Limitations in O<sub>2</sub> supply however, undesirably restricted the levels of % dO<sub>2</sub> present in the medium to <5%, creating an almost anaerobic environment which stimulated the accumulation of high lactate levels reaching 6 g L<sup>-1</sup> at 120 culture hours as shown in ESI Fig. S3.† Evident signs of cellular respiration were further detected until culture harvest at 288 culture hours as a consequence of minimal inlet gas flow-rate variations whereby variations of 0.3% (v/v) for O<sub>2</sub> and 0.4% (v/v) for CO<sub>2</sub> were measured between inlet and outlet signals, suggesting that cell viability was extended possibly as a result of increased nutrient supplementation throughout the culture. The variable composition of the gas supplied to the culture rendered the accurate profiling of CDC, OXC and RQ trends challenging due to an increase in signal noise, which was particularly evident for CDC values as a result of variations in CO<sub>2</sub> mass transfer, thereby requiring averaging of the MS-generated respiratory data at 6 hour time intervals to smoothen signals for CDC, OXC and RQ as illustrated in Fig. 4(B). Stabilization of the gas composition between 87 and 120 culture hours facilitated the visualization of a clear drop in RQ value from 1.1 to 0.7 at 120, 200, and 250 hours indicative of a cellular metabolic switch since it concurred with the depletion of glucose as illustrated in ESI Fig. S3,† similarly to what had been observed in the previously described batch culture B-1 illustrated in Fig. 3(B). A correlation between increases in RQ values and feed additions performed at 96, 168 and 216 culture hours was further visualised. The feed added

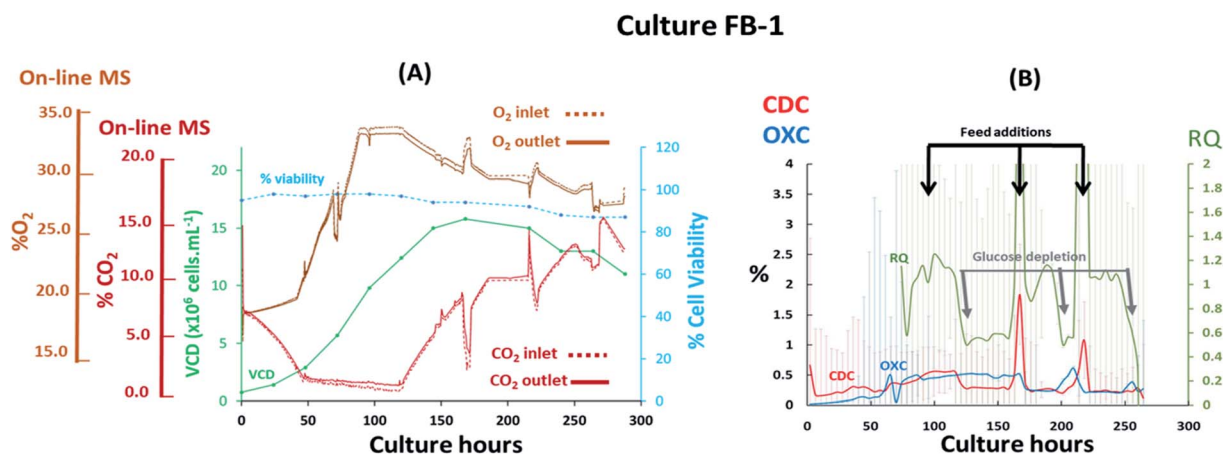


Fig. 4 Profiles of a fed-batch CHO-K1 cell culture, identified as FB-1, illustrating (A) the correlation between off-gas respiratory profiles, obtained by magnetic sector MS, and cell growth profiles obtained from off-line measurements; (B) overlay of CDC, OXC and RQ values, obtained by magnetic sector MS illustrating the impact of feeding events performed at 96, 168 and 216 culture hours on RQ values. Respiratory CDC, OXC and RQ data was averaged from measurements at 6 hour intervals and colour coded error bars from standard deviations were included.

contained a proprietary mixture of nutrients which included glucose, as determined from off-line analysis, thereby contributing to the increases in RQ values which returned to  $\sim 1$  after feeding.

### 3.4 Assessment of sterile barrier integrity by MS

The on-line integration of highly sensitive magnetic sector MS instrumentation with bioreactors provided real-time information on the integrity of essential sterile barriers. The removal of the  $dO_2$  probe, previously described in Section 3.1, which was performed to deliberately contaminate the vessel is unlikely to be the cause of contamination in real process scenarios however, it provided evidence that the occurrence of gaps within the sterile barrier, which can potentially occur due to crack formation or imperfect welds among transfer lines, can be identified by MS and correlated in real-time to process events as they provide an escape route for the exhaust gas which disrupts the stability of the stream directed towards the MS. The formation of an opening on the headplate yielded a flow disruption of the exhaust-gas stream towards the RMS which was detectable in real-time as it resulted in a small but significant drop in the  $CO_2$  values measured from the off-gas at 204 hours, decreasing from 4.90% (v/v) to 4.80% (v/v) as illustrated in Fig. 2. The off-gas MS analyzer was therefore found to be suitable for the determination of undesirable gas escape routes formed if sterile boundaries become compromised which could potentially occur for example due to the formation of cracks along sampling or feeding lines.

Exhaust filter clogging can also occur during cultures as a result of condensate build-up which can yield undesirable pressure increases within the vessels. Typically, the structural integrity of filters would only be verified during bioreactor build-up phases upon pressurizing the filter housing by pumping in compressed air and ensuring that the achieved pressures match nominal values. However, such test does not account for potential issues which could occur during the process. Indeed, partial obstructions on the off-gas transfer line were often visualized as a consequence of condensate build-up on the exhaust filter positioned after the condensate catch-pot, producing abnormal spikes in the exhaust-gas flow-rate measurement which were not attributable to corresponding variations of the inlet gas flow rates as shown in Fig. 5 at 168 culture hours. The geometry of the filter and corresponding surface area were found to influence the propensity to clog which was particularly problematic when filters of 37 mm in diameter were implemented while disruption effects were not observed when replaced by filters of 50 mm diameters.

Further valuable process related information was obtained upon monitoring the flow-rate measurements of the inlet and off-gas streams as determined by the RMS. A decrease in the exhaust-gas flow-rates was visualised in culture FB-1 between 50–60 culture hours, as shown in Fig. 5, with a corresponding increase of the inlet gas flow-rate reaching the MS, therefore suggesting that at this time point the gas supply was primarily directed towards the RMS rather than the bioreactor. A possible explanation was attributed to the increase in cellular biomass

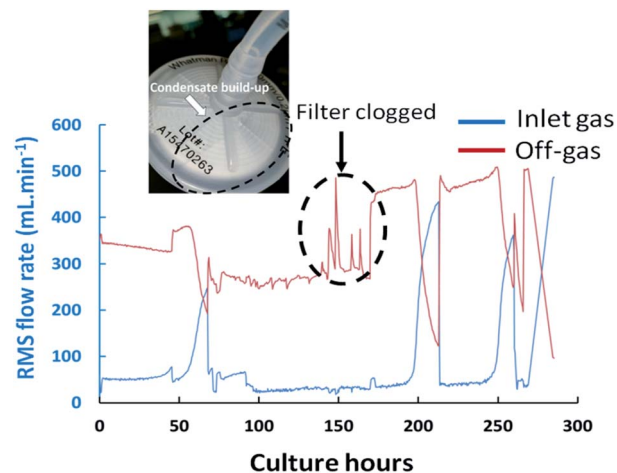


Fig. 5 Flow-rate values measured by the RMS within the magnetic sector MS for inlet and outlet gas streams during the fed-batch cultures FB-1 illustrating disruptions in the inlet gas flow rates, and consequently outlet gas flow-rates, at 68, 213 and 262 culture hours attributed presumably to the increased resistance to gas flow within the bioreactor due to biomass increase. The disturbance at 168 hours was attributed to the presence of partial blockages on the exhaust line filter.

within the bioreactor over time which led to a higher resistance to flow for the supplied gas. Frequent adjustments of the flow-meter back-pressure regulation valves were subsequently required to re-direct the supplied gas stream towards the culture, shown in Fig. 5, producing clear disturbances in the measured  $O_2$  and  $CO_2$  profiles observable at 68, 213 and 262 culture hours in Fig. 4(A).

The clear limitations observed regarding the gas delivery methods in the V1 MS-bioreactor configuration were counteracted by removing the flow diversion mechanism required for directing a portion of the bioreactor's inlet gas towards the RMS. Instead, an analogue signal receiver was integrated as part of a subsequent (V2) configuration, shown in Fig. 1(B), whereby the composition of the inlet gas supplied to the culture was calculated by the GasWorks software automatically upon accurate characterization of the air composition introduced into the culture, which was determined by running a separate line from the air supply directly to the MS analyzer, and analogue transfer of flow-rate information for each individual gas from the G3Lab setup, resulting in the improved stability of the exhaust-gas flow-rate as illustrated in ESI Fig. S2.† A further benefit of the V2 configuration involved the increased amount of available sampling ports on the MS which would be now capable of potentially monitoring 15 different bioreactors simultaneously assuming that they all shared the same air supply.

### 3.5 Impact of process variables on off-gas profiles

Fed-batch cultures performed subsequently to the implementation of the V2 MS-bioreactor configuration were aimed at assessing the performance of the MS analyser for mammalian cell culture monitoring upon alteration of the culture temperature conditions and glucose supplementation, implemented



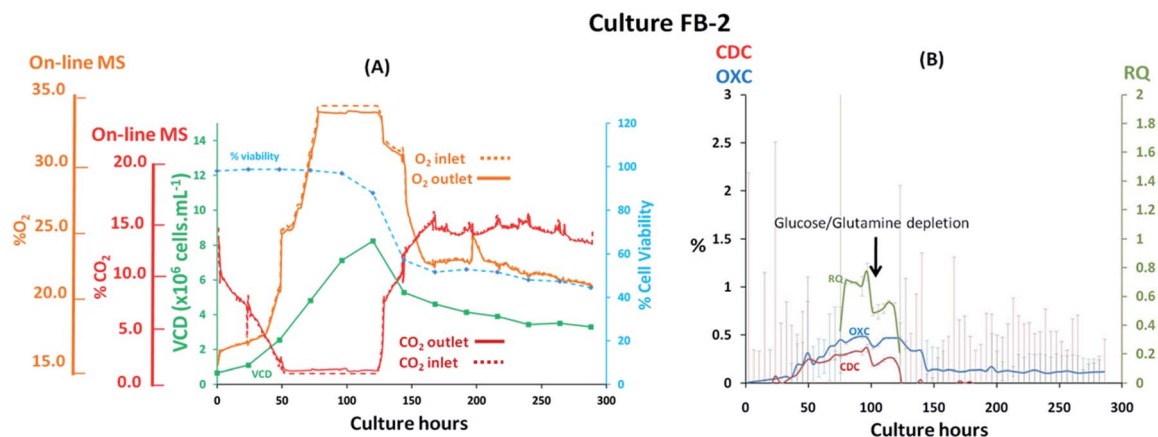


Fig. 6 Cell growth and respiratory profiles of a CHO-K1 fed-batch cell culture which involved the implementation of a temperature down-shift, identified as FB-2, illustrating (left) the correlation between off-gas respiratory profiles, obtained by magnetic sector MS, and cell growth profiles obtained from off-line measurements; (right) overlay of CDC, OXC and RQ values, obtained by magnetic sector MS illustrating the impact on RQ values upon depletion of glucose/glutamine. Respiratory CDC, OXC and RQ data was averaged from measurements at 6 hour intervals and colour coded error bars from standard deviations were included.

as part of cultures FB-2 and FB-3 respectively, which clearly affected culture performance as detected by off-gas measurements show in Fig. 6 and 7. Similar peak cell densities of  $8 \times 10^6$  cells per  $\text{mL}^{-1}$  were achieved in both FB-2 and FB-3 cultures which however, were approximately half of the density values observed in culture FB-1. Despite the similar aeration conditions implemented among the three fed batch cultures described, illustrated in ESI Fig. S1,<sup>†</sup> the elevated air flow rates introduced into cultures FB-2 and FB-3 promoted bubble formation, therefore causing excessive cell shear stress<sup>40</sup> which produced noticeable changes in cell growth behaviour, resulting in decreased culture longevity. Instead, the aeration rates which were introduced in fed-batch culture FB-1 were considerably lower than expected, as observed from the off-gas flow-rate profile illustrated in Fig. 5, since they were affected by the aforementioned limitations of the V1 MS-bioreactor

configuration, which presumably contributed to the prolonged cell viabilities observed. Similarities among cell growth curves and respiratory profiles were observed for fed-batch cultures FB-2 and FB-3 until 122 culture hours, as seen in Fig. 6(A) and 7(A), since identical process conditions were implemented until this time point. A stable gas composition was implemented in both fed-batch cultures from 75 culture hours upon limiting the flow-rate of supplemented  $\text{O}_2$  as previously performed in culture FB-1 to facilitate the accurate quantification of respiratory-induced activity as confirmed by a measured difference between inlet and off-gas signals of 0.4% (v/v) and 0.5% (v/v) for  $\text{O}_2$  in cultures FB-2 and FB-3 respectively at 100 culture hours, with a corresponding 0.2% (v/v) and 0.3% (v/v) increase in  $\text{CO}_2$  levels. Average RQ values of 0.75 were determined between 80–100 culture hours in both fed-batch cultures, shown in Fig. 6(B) and 7(B) respectively, which were considerably lower to what had

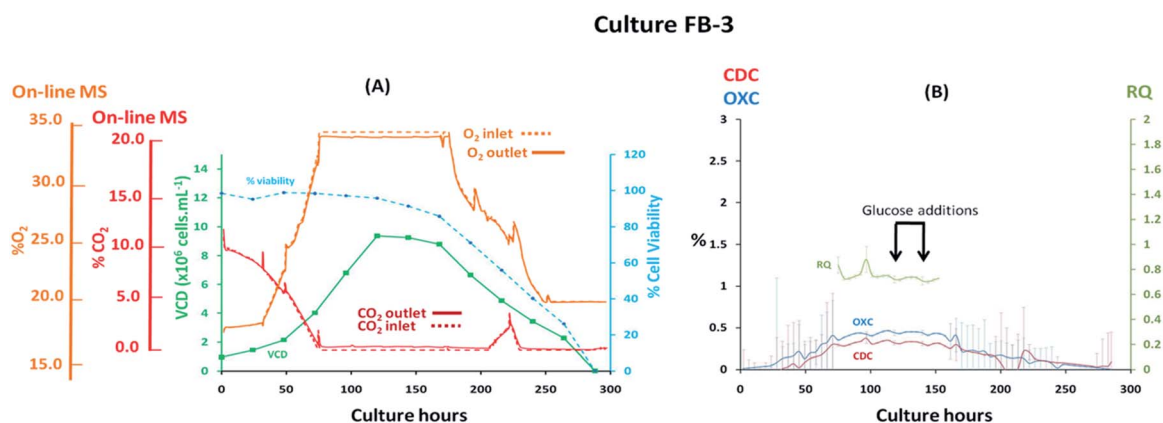


Fig. 7 Cell growth and respiratory profiles of a CHO-K1 fed-batch cell culture which involved glucose supplementation, identified as FB-3, illustrating (left) the correlation between off-gas respiratory profiles, obtained by magnetic sector MS, and cell growth profiles obtained from off-line measurements; (right) overlay of CDC, OXC and RQ values, obtained by magnetic sector MS illustrating the impact on RQ values upon glucose supplementation. Respiratory CDC, OXC and RQ data was averaged from measurements at 6 hour intervals and colour coded error bars from standard deviations were included.

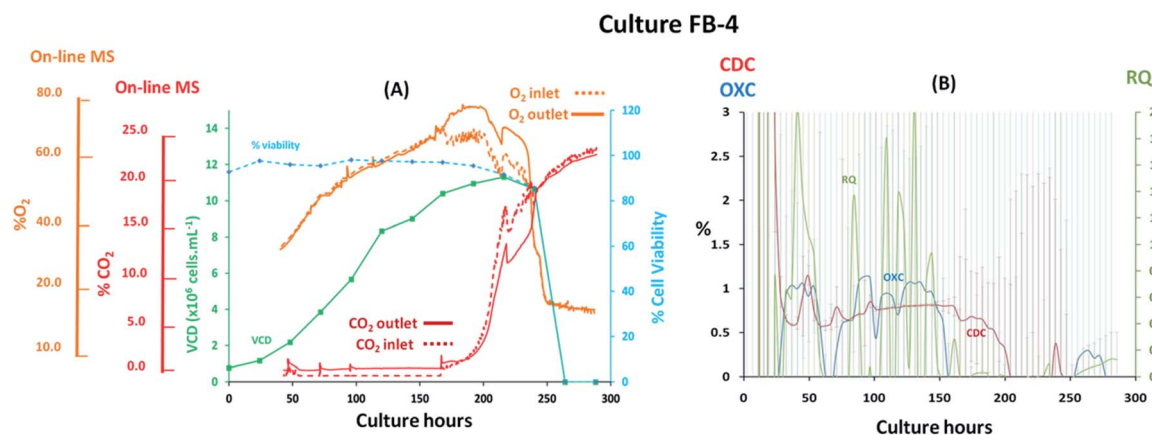


Fig. 8 Cell growth and respiratory profiles of a CHO-K1 fed-batch cell culture which involved maintaining %dO<sub>2</sub> levels at 40–50%, identified as FB-4, illustrating (left) the correlation between off-gas respiratory profiles, obtained by magnetic sector MS, and cell growth profiles obtained from off-line measurements; (right) overlay of CDC, OXC and RQ values, obtained by magnetic sector MS illustrating the impact on RQ values upon continuous fluctuations in gas supply due to O<sub>2</sub> supplementation. Respiratory CDC, OXC and RQ data was averaged from measurements at 6 hour intervals and colour coded error bars from standard deviations were included.

been observed in cultures B-1 and FB-1 therefore indicative of the absence of a predominantly carbohydrate-based metabolism. Values for the RQ in this range are instead indicative of fatty acid oxidation, although this could not be verified by off-line quantitative assays. A further drop in RQ value to 0.56 was observed at 100 hours in culture FB-2, shown in Fig. 6(B), occurring simultaneously to glucose/glutamine depletion, followed by a drop in cell viability to 88% at 120 hours which decreased further to 55% at 144 hours. The implementation at this point of a culture temperature drop from 37 °C to 32 °C did not impact off-gas measurements contrary to expectations since a consequent increase in CO<sub>2</sub> solubility was anticipated to yield a decrease in measured CO<sub>2</sub> levels from the off-gas. The composition of both inlet and off-gas streams was identical from 144 to 288 hours and no respiratory activity could not be visualised as a result of the low cell viability present which therefore resulted in inaccurate RQ data during this period (not illustrated). However, the decreased temperature conditions prevented further drops in cell viability, which remained stable until the point of harvest at 288 hours, and produced an increase in protein yield commonly observed in CHO cell cultures<sup>41</sup> illustrated in the ESI Fig. S4.† A process change involving the supplementation of glucose was performed in culture FB-3 at 120 and 144 culture hours, as shown in Fig. 7(B), which prevented the rapid deterioration of culture conditions observed in culture FB-2 as confirmed by the stability of the RQ values which were maintained at 0.75 until 160 culture hours. The determined outcome was not surprising since cells could divert more energy to growth therefore resulting in a likely change of metabolism as confirmed by visualised disturbances in both the OXC and CDC profiles at the two feeding intervals. However, the increase in glucose levels combined with the anaerobic conditions present due to O<sub>2</sub> flow-rate limitations resulted in the high accumulation of lactate which reached concentrations of 12 g L<sup>-1</sup> in culture FB-3, almost double the levels observed in cultures FB-1 and FB-2, as shown in ESI

Fig. S3.† A fourth fed-batch culture, identified as FB-4 and shown in Fig. 8, was evaluated to determine the effects of rapid changes in inlet gas composition on off-gas profiles which were not stabilized as in the previously evaluated fed-bath cultures. In culture FB-4, aeration rates were considerably decreased to 0.1 L min<sup>-1</sup> to minimize shear stress on the cells, yielding considerably reduced levels of accumulated lactate which peaked 2.4 g L<sup>-1</sup> at 120 hours as shown in ESI Fig. S3.† A shift in lactate metabolism was further visualized from 120 culture hours as it became a carbon nutrient source until 250 hours, revealing a positive effect on antibody production as observed in the ESI Fig. S4.† Variable quantities of O<sub>2</sub> and CO<sub>2</sub> were introduced throughout the culture as necessary to maintain dO<sub>2</sub> levels between 40–50% saturation and pH values at 7.0. However, the low initial gas flow-rates supplied to the culture prevented the satisfactory characterization of the off-gas composition due to the consequently low off-gas flow-rates reaching the MS which necessitates of values between 200–500 mL min<sup>-1</sup> for accurate measurements. The rate of aeration was marginally increased to 0.15 L min<sup>-1</sup> after 24 culture hours in effort to consequently increase the flow-rates of the off-gas. However, satisfactory flow-rate conditions were achieved only after 48 culture hours as air became enriched with O<sub>2</sub>. Clear signs of respiratory activity were detected from off-gas O<sub>2</sub> measurements shown in Fig. 8(A) despite the large concentration variations observed in O<sub>2</sub> supply which increased from 33% to 67% during 48–166 culture hours. Respiratory signs were particularly evident during phases when linearity in the O<sub>2</sub> supply gradient was achieved. For example, a 0.63% (v/v) decrease in O<sub>2</sub> and a 0.64% (v/v) increase in CO<sub>2</sub> was visualised at 80 culture hours involving a viable cell density of 4 × 10<sup>6</sup> cells per mL<sup>-1</sup>. However, respiratory-induced activity was primarily visualised from CO<sub>2</sub> measurements from 48 to 160 culture hours due to lower variations in the signal intensity scale as established from the previously characterised fed-batch cultures FB-1, FB-2 and FB-3. The continuous variations in the

O<sub>2</sub> inlet flow supply required for the preservation of % dO<sub>2</sub> levels between 40–50% were particularly significant during 160–250 culture hours, as illustrated from the bioreactor gas flow-rate profiles shown in the ESI Fig. S1,† and resulted in large off-gas measurement errors in the same time interval which impacted predominantly the determination of meaningful OXC values, thereby resulting in unstable RQ data as shown in Fig. 8(B), and prevented the visualization of further cellular respiratory activity.

## 4 Conclusions

Real-time monitoring of mammalian cell culture processes was performed through off-gas characterization upon the on-line integration of a magnetic sector MS analyser with benchtop bioreactors. Critical process-related information, including variations in culture medium temperature during medium hold stages and alterations within the sterile barriers were readily identified from disturbances in the off-gas profile signals which can be extremely beneficial when root cause analysis investigations are performed to explain unaccounted variations in process performance. The rapid detection of contamination events by MS was demonstrated from the visualization of clear microbial respiratory activity signs, revealing similar performance to % dO<sub>2</sub> measurements obtained *in situ*. Respiratory activity from CHO cell processes was visualised from the lag phase depending on the experimental configuration implemented, involving relatively low VCDs of  $\sim 1 \times 10^6$  cells per mL<sup>-1</sup>. A significant drop in off-gas O<sub>2</sub> concentrations of 0.04% (v/v) was visualized at this time point which would be impossible to detect using less sensitive paramagnetic analyzers due to their inferior precision of typically  $\pm 0.2\%$  (v/v). Clear shifts in RQ values from mammalian cell culture processes were visualised upon determination of respiratory profiles by MS and correlated with variations in substrate consumptions measured off-line. However, rapid changes in gas supply composition to the culture rendered the monitoring of mammalian cell respiratory activity challenging particularly during stationary phases when the cell density level and consequent O<sub>2</sub> demand were high. A possible solution for this issue would involve the implementation of a mass-flow controller prior to the MS to stabilize the off-gas flow however, the efficacy of this setup could not be yet verified. While the MS requires a significant initial capital investment, it integrates multiple functionalities within a single platform which would otherwise require multiple standalone consumables and alternative equipment. Relative to in-line probes for example, the MS analyser is not subjected to stressful autoclaving conditions which affect the lifespan of probes, and can be configured to monitor up to 15 bioreactors simultaneously based on the non-invasive V2 configuration, therefore being particularly beneficial for process development applications. The combination of these features with the high signal stability and infrequent calibration requirements of the magnetic sector MS translate into an attractive process monitoring solution particularly as biopharmaceutical manufacturing operations shift from traditional fed-batch to continuous modes.

## Conflicts of interest

The authors declare no conflict of interest. Mr Graham Lewis, Mr Graham Josland and Mr Daniel Merriman are employees of Thermo Fisher Scientific, Ion Path, Road Three, Winsford, CW7 3 GA, United Kingdom.

## Acknowledgements

The authors would like to thank Enterprise Ireland for funding the described studies under grant IP/2017/0449.

## References

- 1 M. Jenzsch, C. Bell, S. Buziol, F. Kepert, H. Wegele and C. Hakemeyer, *Adv Biochem Eng Biotechnol*, 2018, **165**, 211–252.
- 2 F. Li, N. Vijayasankaran, A. Shen, R. Kiss and A. Amanullah, *mAbs*, 2010, **2**, 466–479.
- 3 M. Streefland, D. E. Martens, E. C. Beuvery and R. H. Wijffels, *Eng. Life Sci.*, 2013, **13**, 212–223.
- 4 A. P. Teixeira, R. Oliveira, P. M. Alves and M. J. T. Carrondo, *Biotechnol Adv*, 2009, **27**, 726–732.
- 5 L. Zhao, H.-Y. Fu, W. Zhou and W.-S. Hu, *Eng. Life Sci.*, 2015, **15**, 459–468.
- 6 C. Altamirano, J. Berrios, M. Vergara and S. Becerra, *Electron J Biotechnol*, 2013, **16**, 10.
- 7 B. C. Mulukutla, A. Yongky, S. Grimm, P. Daoutidis and W.-S. Hu, *PLoS One*, 2015, **10**, e0121561.
- 8 T. Bachinger, U. Riese, R. Eriksson and C.-F. Mandenius, *J. Biotechnol.*, 2000, **76**, 61–71.
- 9 L. Fitzpatrick, H. A. Jenkins and M. Butler, *Appl. Biochem. Biotechnol.*, 1993, **43**, 93–116.
- 10 C. M. Kussow, W. Zhou, D. M. Gryte and W.-S. Hu, *Enzyme Microb. Technol.*, 1995, **17**, 779–783.
- 11 Z. L. Xiu, W. D. Deckwer and A. P. Zeng, *Cytotechnology*, 1999, **29**, 159–166.
- 12 S. Aiba, S. Nagai and Y. Nishizawa, *Biotechnol. Bioeng.*, 1976, **18**, 1001–1016.
- 13 R. M. Dekkers and M. Voetter, *IFAC Proceedings Volumes*, 1985, **18**, 103–110.
- 14 X. Li, C. Yu, J. Yao, Z. Wang and S. Lu, *Front Bioeng Biotech*, 2018, **5**, 1–11.
- 15 J. Xiao, Z. Shi, P. Gao, H. Feng, Z. Duan and Z. Mao, *Bioprocess Biosyst. Eng.*, 2006, **29**, 109–117.
- 16 H. P. J. Bonarius, C. D. de Gooijer, J. Tramper and G. Schmid, *Biotechnol. Bioeng.*, 1995, **45**, 524–535.
- 17 G. Lovrecz and P. Gray, *Cytotechnology*, 1994, **14**, 167–175.
- 18 H. H. J. Bloemen, L. Wu, W. M. van Gulik, J. J. Heijnen and M. H. G. Verhaegen, *AIChE J.*, 2003, **49**, 1895–1908.
- 19 S. Winckler, R. Krueger, T. Schnitzler, W. Zang, R. Fischer and M. Biselli, *Bioprocess Biosyst. Eng.*, 2014, **37**, 901–912.
- 20 M. Aehle, A. Kuprijanov, S. Schaepe, R. Simutis and A. Lubbert, *Biotechnol. Lett.*, 2011, **33**, 2103–2110.
- 21 M. Aehle, S. Schaepe, A. Kuprijanov, R. Simutis and A. Lubbert, *J. Biotechnol.*, 2011, **153**, 56–61.
- 22 W. Zhou and W. S. Hu, *Biotechnol. Bioeng.*, 1994, **44**, 170–177.

- 23 W. Zhou, J. Rehm and W. S. Hu, *Biotechnol. Bioeng.*, 1995, **46**, 579–587.
- 24 P. A. Ruffieux, U. von Stockar and I. W. Marison, *J. Biotechnol.*, 1998, **63**, 85–95.
- 25 V. Singh, *Biotechnol. Bioeng.*, 1996, **52**, 443–448.
- 26 B. Frahm, H.-C. Blank, P. Cornand, W. Oelßner, U. Guth, P. Lane, A. Munack, K. Johannsen and R. Pörtner, *J. Biotechnol.*, 2002, **99**, 133–148.
- 27 H.-Y. Goh, M. Sulu, H. Alosert, G. L. Lewis, G. D. Josland and D. E. Merriman, *Bioproc. Biosyst. Eng.*, 2020, **43**, 483–493.
- 28 A. Oezemre and E. Heinzle, *Cytotechnology*, 2001, **37**, 153–162.
- 29 U. Behrendt, S. Koch, D. D. Gooch, U. Steegmans and M. J. Comer, *Cytotechnology*, 1994, **14**, 157–165.
- 30 P. Turner, S. Taylor, E. Clarke, C. Harwood, K. Cooke and H. Frampton, *TrAC, Trends Anal. Chem.*, 2004, **23**, 281–287.
- 31 M. Naciri, D. Kuystermans and M. Al-Rubeai, *Cytotechnology*, 2008, **57**, 245–250.
- 32 R. Wiebe and V. L. Gaddy, *J. Am. Chem. Soc.*, 1940, **62**, 815–817.
- 33 P. N. Royce, *Biotechnol. Bioeng.*, 1992, **40**, 1129–1138.
- 34 C. A. Perkowski, *J. Parenter. Sci. Technol.*, 1990, **44**, 113–117.
- 35 H. Siegumfeldt, K. Bjorn Rechinger and M. Jakobsen, *Appl. Environ. Microbiol.*, 2000, **66**, 2330–2335.
- 36 M. Sperandio and E. Paul, *Biotechnol. Bioeng.*, 1997, **53**, 243–252.
- 37 J. Neermann and R. Wagner, *J. Cell. Physiol.*, 1996, **166**, 152–169.
- 38 T. L. Place, F. E. Domann and A. J. Case, *Free Radical Biol. Med.*, 2017, **113**, 311–322.
- 39 M. Flinck, S. H. Kramer and S. F. Pedersen, *Acta Physiol.*, 2018, **223**, e13068.
- 40 W. Hu, C. Berdugo and J. J. Chalmers, *Cytotechnology*, 2011, **63**, 445–460.
- 41 M. Mason, B. Sweeney, K. Cain, P. Stephens and T. S. Sharfstein, *Antibodies*, 2014, **3**, 253–271.